DEFENCE R&D DÉFENSE

Analysis of the Radiation Environment Effects on Electronic Components in Near-Earth Orbits

L. Varga, E. Horvath and T. Cousins
Defence Research Establishment Ottawa

Defence R&D Canada
DEFENCE RESEARCH ESTABLISHMENT OTTAWA

TECHNICAL MEMORANDUM
DREO TM 2000-071
November 2000

National Defence Défense nationale

Canada

ABSTRACT

The radiation environments at two low altitude orbits have been calculated with the NASA space environment models and codes AP8/AE8, Vette, and CREME. LET spectra and device upset rates for various solar activity scenarios have been determined. Dose deposition into silicon targets as a function of Aluminum shielding thickness has been also calculated with a Monte Carlo code. The results indicate that parameters such as orbit altitude, shielding thickness, and solar activity strongly affect the SEU rates.

RÉSUMÉ

L'environnement de rayonnement à deux orbites de basse altitude a été calculé en utilisant des modèles d'environnement e l'espace de NASA's et code AP8/AE8, Vette et CRÈME. Les spectres LET et les cadences bouleversées de dispositif pour différents scénarios solaires d'activité avoir été déterminé. Le dépôt de dose dans des cibles de silicium en fonction d'épaisseur d' armature d'aluminium a été également calculé en utilisant un code de Monte Carlo. Les résultats indiquent que les paramètres tels que l'altitude d'orbite, protégeant l'épaisseur et l'activité solaire affectent fortement les cadences de SEU.

EXECUTIVE SUMMARY

The radiation environment and its effect on space vehicle electronic components have been determined for two low altitude orbits. The orbits selected were polar/circular with altitudes of 600km and 1100km. The orbit parameters were specified by TTRDP.

The NASA Space environment codes AP8/AE8, Vette, and CREME were used to obtain radiation spectra, LET spectra and device upset rates for various solar activity scenarios. The effect of aluminum shielding on the dose deposition and electronic device upset rates was also calculated. The devices were evaluated according to critical charge magnitude, and the size of the sensitive volume. The former parameter refers to the amount of charge required to upset the device status; the latter parameter is the region inside the device with an electric field; for example a PN junction. Dose deposition into silicon targets as a function of Aluminum shielding thickness was calculated with a Monte Carlo code.

The calculations indicate that parameters such as orbit altitude and solar activity strongly affect the dose deposition and the upset rates of satellite electronic components. It was also determined that only about the first two to three millimeters of Aluminum shielding is important; after that the Aluminum thickness shielding effect becomes less significant.

[Varga, L., Horvath, E. and Cousins T., 2000, Analysis of the Radiation Environment Effect on Electronic Components in Near-Earth Orbits, Tech. Mem. No. TM 2000-071, DREO]

SOMMAIRE

L'environnement de rayonnement et l'effet sur les composants électroniques d'un véhicule spatial ont été déterminés pour deux orbites de basse altitude. Les orbites choisies étaient polar/circular avec des altitudes de 600km et de 1100km. Les paramètres d'orbite ont été indiqués par TTRDP.

L'environnement de l'espace de la NASA code AP8/AE8, Vette, et la CRÈME ont été employées pour obtenir des spectres de rayonnement, des spectres LET et des cadences bouleversées de dispositif électronique pour différents scénarios solaires d'activité. L'effet de l'aluminium protégeant sur les cadences bouleversées de dépôt et de dispositif de dose a été également calculé. Les dispositifs ont été évalués selon l'importance critiquede charge, et la taille du volume sensible. L'ancien paramètre se rapporte à la quantité de charge exigée pour déranger le mode de dispositif; le dernier paramètre est la région à l'intérieur du dispositif qui contient le champ électrique; comme la jonction de PN. Le dépôt de dose dans des cibles de silicium en fonction d'épaisseur d' armature d'aluminium a été calculé en utilisant un code de Monte Carlo.

Les calculs indiquent que les paramètres tels que l'altitude d'orbite et l'activité solaire affectent fortement le dépôt de dose et les cadences bouleversées des composants électroniques satellites. On l'a également déterminé que le seul environ les deux premiers à trois millimètres d'armature d'aluminium est important, ensuite cela que l'effet d' armature d'épaisseur en aluminium devient moins significatif.

[Varga, L., Horvath, E. and Cousins T., 2000, Analysis of the Radiation Environment Effect on Electronic Components in Near-Earth Orbits, Tech. Mem. No. TM 2000-071, DREO]

TABLE OF CONTENTS

ABSTRACT.....iii

RESUME.....iii

EXECUTIVE SUMMARY.....v

SOMMAIRE EXECUTIF.....v

TABLE OF CONTENTS.....vii

LIST OF FIGURES.....ix

LIST OF TABLES.....xi

1. Introduction.....1

2. Trapped Radiation.....2

3. Cosmic Rays.....6

4. LET Spectrum.....6

5. Shielding Effect on LET Spectrum.....12

6. Upset Rates.....14

7. Dose Deposition.....16

8. Summary.....17

9. References.....17

LIST OF FIGURES

Figure 1. Trapped differential electron spectra. 4

Figure 2. Trapped differential proton spectra. 4

Figure 3. Spatial distribution of the trapped electron flux at the 1100km altitude (a) and the 600km altitude (b). 5

Figure 4. Spatial distribution of the trapped proton flux at the 1100km altitude (a) and the 600km altitude (b). 5

Figure 5. Proton, Helium, Oxygen and Iron spectra for galactic cosmic rays at the altitude of 600km. 7

Figure 6. Proton, Helium, Oxygen and Iron spectra for galactic cosmic rays including an average solar flare particle flux at the altitude of 600km. 7

Figure 7. Proton, Helium, Oxygen and Iron spectra for galactic cosmic rays at the altitude of 1100km. 8

Figure 8. Proton, Helium, Oxygen and Iron spectra for galactic cosmic rays including an average solar flare particle flux at the altitude of 1100km. 8

Figure 9. LET spectrum for the specified interplanetary conditions for the 600km circular orbit. 11

Figure 10. LET spectrum for the specified interplanetary conditions for the 600km circular orbit. 11

Figure 11. Effect of Aluminum shielding thickness on the LET spectrum of galactic cosmic rays at the altitude of 600km. 12

Figure 12. Effect of Aluminum shielding on the LET spectrum of galactic cosmic rays including an ordinary solar flare component at the altitude of 600km. 13

Figure 13. Effect of Aluminum shielding thickness on the LET spectrum of galactic cosmic rays at the altitude of 1100km. 13

Figure 14. Effect of Aluminum shielding on the LET spectrum of galactic cosmic rays including an ordinary solar flare component at the altitude of 1100km. 14

Figure 15. The critical volume size and the critical charge magnitude effect on device upset rates at 1100km altitude. 15

Figure 16. Shielding and solar activity effect on device upset rates at the 1100km altitude. 15

Figure 17. Shielding and solar activity effect on device upset rates at the 600km altitude. 16

LIST OF TABLES

Table 1. Geomagneticaly Trapped Differential Electron Spectra. 2

Table 2. Geomagneticaly Trapped Differential Proton Spectra. 3

Table 3. Differential galactic cosmic ray flux (particles m^{-2} s^{-1} $ster^{-1}$ $(MeV/u)^{-1}$ at the altitude of 600km (four elements shown). 9

Table 4. Differential galactic cosmic ray flux including an average intensity solar flare component (particles m^{-2} s^{-1} $ster^{-1}$ $(MeV/u)^{-1}$ at the altitude of 600km (four elements shown). 9

Table 5. Differential galactic cosmic ray flux (particles m^{-2} s^{-1} $ster^{-1}$ $(MeV/u)^{-1}$ at the altitude of 1100km (four elements shown). 10

Table 6. Differential galactic cosmic ray flux including an average intensity solar flare component (particles m^{-2} s^{-1} $ster^{-1}$ $(MeV/u)^{-1}$ at the altitude of 1100km (four elements shown). 10

Table 7. Dose deposition rates (rad day^{-1}) at the altitude of 600km. 16

Table 8. Dose deposition rates (rad day^{-1}) at the altitude of 1100km. 17

1. INTRODUCTION

Critical to the survivability and mission success of any space-based platform, is that it be able to withstand the deleterious effects of ionizing radiation on the system electronics. The radiation environment to which a space-platform is subjected is orbit specific; the magnetosphere of the Earth affects the charged particle spectrum encountered in near-earth orbits. Solar activity further affects the temporal variations either long term, as evidenced by cyclical variation in solar activity, or in the short term, by the effects of solar flares or coronal holes. It is desirable, therefore, to have a means of predicting the radiation environment that a spacecraft will likely encounter over the duration of its mission. This information can then be utilized during the specification, design, and testing phases of the development a space vehicle, to ensure that radiation hardness survivability criteria can be met.

Total dose effects, single-event upsets, and electrostatic charging/discharging (ESD) are the primary radiation effects on electronics of interest to the spacecraft system designer. Material degradation, such as surface erosion, due to the synergistic effects of heavy ions and ultraviolet radiation (ex. LDEF mission) are also important and, among other things, affect solar array covers and thermal blankets.

Space radiation environmental models and computational methods for estimating total dose and single-event upset (SEU) rates have been developed and in use for several decades. As part of the development of in-house expertise in Space Radiation Effects at Defence Research Establishment Ottawa (DREO), publicly available computer codes (primarily from NASA and RSIC) applicable to space radiation effects have been obtained and utilized. To further enhance the computational capability for estimating radiation effects on space-based electronic platforms, for arbitrary orbits, additional in-house development of models applicable to electrostatic charging and dose deposition into complex 3D objects has also been undertaken and completed.

In this work we determine a number of parameters associated with the space environment in general and space radiation environment in particular. The results presented pertain to two circular orbits, namely, an orbit with 600km altitude and one with 1100km altitude. The inclination angles of the two orbits are 98° and 85°, respectively (specified by TTRDP). Description of the computer programs will be kept to a minimum (described in greater detail elsewhere); however, some application capabilities will be highlighted.

2. TRAPPED RADIATION

The motion of charged particles in the earth's magnetosphere is governed by the magnitude and relative direction of the earth's magnetic field to the particle velocity vector. The distribution of the trapped radiation in the magnetosphere is best described in a "B-L coordinate system" introduced by McIlwain, et al[1]. The coordinate L is called McIllwain's magnetic shell parameter and B is the magnetic field strength.

The trapped electron model, designated AE8, was used to obtain the trapped electron spectra for the two orbits; for protons, the AP8 model has been used. Both AP8 and AE8 models provide an average spectrum for the given orbit, based on measurements obtained by a number of satellites over a period of several years. The trapped proton model (AP8) is applicable in the energy range of 100keV to 400MeV, the AE8 model is valid from 40keV to 6MeV. The computer programs "ORBIT" and "VETTE", which implement these models, are available from the National Space Science Data Center at NASA-GFC. The program output consists of differential, integral, and energy-window binned spectra of trapped radiation specific to a given orbit. Additional outputs such as particle flux at each point of an orbit, average integral flux within an L-band, total particle flux/orbit, and others can also be obtained.

The trapped electron and proton spectrum for the two orbits is summarized in Tables 1 and 2.

Table 1. Geomagnetically Trapped Differential Electron Spectra.

Orbit Data: 1) Circular; Altitude = 1100km; Inclination angle = 85 degrees 2) Circular; Altitude =600km; Inclination angle =98 degrees				
Electron energy	**Solar Maximum**		**Solar Minimum**	
	1100km orbit	**600km orbit**	**1100km orbit**	**600km orbit**
(MeV)	**Electrons cm^{-2} day^{-1} MeV^{-1}**		**Electrons cm^{-2} day^{-1} MeV^{-1}**	
5.50E-02	9.09E+11	1.56E+11	4.56E+11	6.81E+10
6.50E-02	8.47E+11	1.43E+11	4.22E+11	6.21E+10
7.50E-02	7.87E+11	1.31E+11	3.89E+11	5.63E+10
8.50E-02	7.33E+11	1.20E+11	3.59E+11	5.12E+10
9.50E-02	6.82E+11	1.11E+11	3.32E+11	4.68E+10
1.25E-01	7.00E+11	1.03E+11	3.52E+11	4.36E+10
3.00E-01	2.57E+11	2.67E+10	7.94E+10	9.61E+09
4.25E-01	1.06E+11	1.14E+10	3.36E+10	4.35E+09
6.00E-01	2.21E+10	3.78E+09	1.08E+10	1.77E+09
8.50E-01	5.93E+09	1.38E+09	3.49E+09	7.26E+08
1.25E+00	1.90E+09	5.56E+08	1.25E+09	3.22E+08
1.75E+00	6.38E+08	2.14E+08	3.97E+08	1.15E+08
2.25E+00	2.62E+08	9.00E+07	1.59E+08	4.72E+07
2.75E+00	1.32E+08	4.27E+07	8.11E+07	2.19E+07
3.50E+00	5.28E+07	2.78E+06	3.12E+07	9.71E+06
4.50E+00	6.63E+06	3.02E+05	4.72E+06	1.94E+06
5.50E+00	6.58E+05	1.02E+04	6.02E+05	1.01E+04

Table 2. Geomagneticaly Trapped Differential Proton Spectra.

Orbit Data: 1)Circular; Altitude = 1100km; Inclination angle = 85 degrees 2) Circular; Altitude =600km; Inclination angle = 98 degrees				
Proton energy	**Solar Maximum**		**Solar Minimum**	
	1100km orbit	**600km orbit**	**1100km orbit**	**600km orbit**
(MeV)	**Protons cm^{-2} day^{-1} MeV^{-1}**		**Protons cm^{-2} day^{-1} MeV^{-1}**	
1.50E-01	1.26E+10	8.49E+08	1.19E+10	9.04E+08
2.50E-01	5.28E+09	3.86E+08	5.38E+09	4.73E+08
3.50E-01	2.33E+09	1.80E+08	2.46E+09	2.42E+08
4.00E-01	6.34E+08	5.01E+07	7.22E+08	8.65E+07
7.50E-01	8.04E+07	5.38E+06	1.11E+08	1.69E+07
2.00E+00	1.02E+07	5.33E+05	1.56E+07	2.49E+06
4.00E+00	3.32E+06	1.49E+05	4.90E+06	6.99E+05
7.50E+00	1.27E+06	5.72E+04	1.72E+06	1.81E+05
1.50E+01	5.08E+05	2.65E+04	6.65E+05	6.06E+04
2.50E+01	2.82E+05	1.84E+04	3.72E+05	3.75E+04
3.50E+01	2.18E+05	1.56E+04	2.93E+05	3.17E+04
4.50E+01	1.90E+05	1.41E+04	2.60E+05	2.87E+04
5.50E+01	1.70E+05	1.32E+04	2.39E+05	2.66E+04
7.00E+01	1.42E+05	1.14E+04	2.02E+05	2.20E+04
9.00E+01	1.19E+05	9.93E+03	1.69E+05	1.81E+04
1.20E+02	8.09E+04	6.71E+03	1.13E+05	1.16E+04
1.50E+02	6.59E+04	5.35E+03	9.18E+04	9.13E+03
1.70E+02	5.40E+04	4.31E+03	7.48E+04	7.28E+03
1.90E+02	4.47E+04	3.63E+03	6.06E+04	5.81E+03
2.20E+02	3.06E+04	2.45E+03	4.07E+04	3.78E+03
250	2.52E+04	1.97E+03	3.35E+04	3.05E+03
280	1.72E+04	1.29E+03	2.28E+04	2.01E+03
330	9.78E+03	6.94E+02	1.29E+04	1.09E+03
380	6.71E+03	4.60E+02	8.78E+03	7.23E+02
450	2.67E+03	1.68E+02	3.44E+03	2.66E+02

In a graphical form, the spectra are presented in Figure 1 and Figure 2, with both solar maximum and minimum shown. Figure 3 (panels a, b) and Figure 4 (panels c, d) provides information about the spatial distribution of the trapped electron flux (E>0.7MeV) and proton flux (E>0.1MeV) intercepting the plane of the two orbits. It is evident that the electron and proton flux is concentrated in the area of the South Atlantic Anomaly, although appreciable electron flux is also observed in the Auroral Oval area in both hemispheres. For protons, the flux contribution from the Auroral Oval regions is negligible. The effect of altitude on the flux magnitude becomes evident when comparing panels (a) and (b) in Figure 3 and panels (c) and (d) in Figure 4. For better visual comparison of the differences between the two orbits, the same scales have been used.

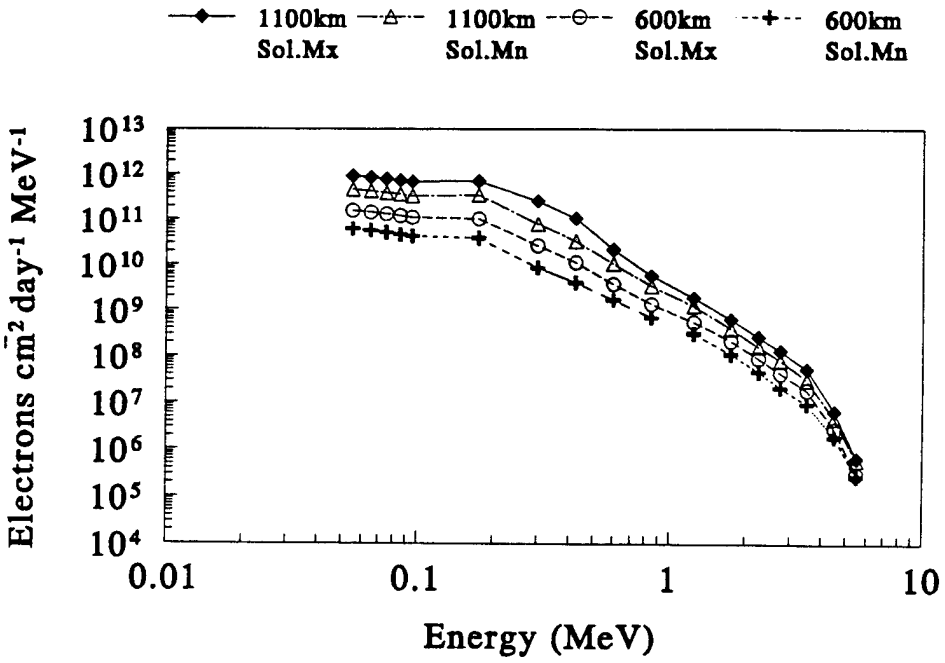

Figure 1. Trapped differential electron spectra.

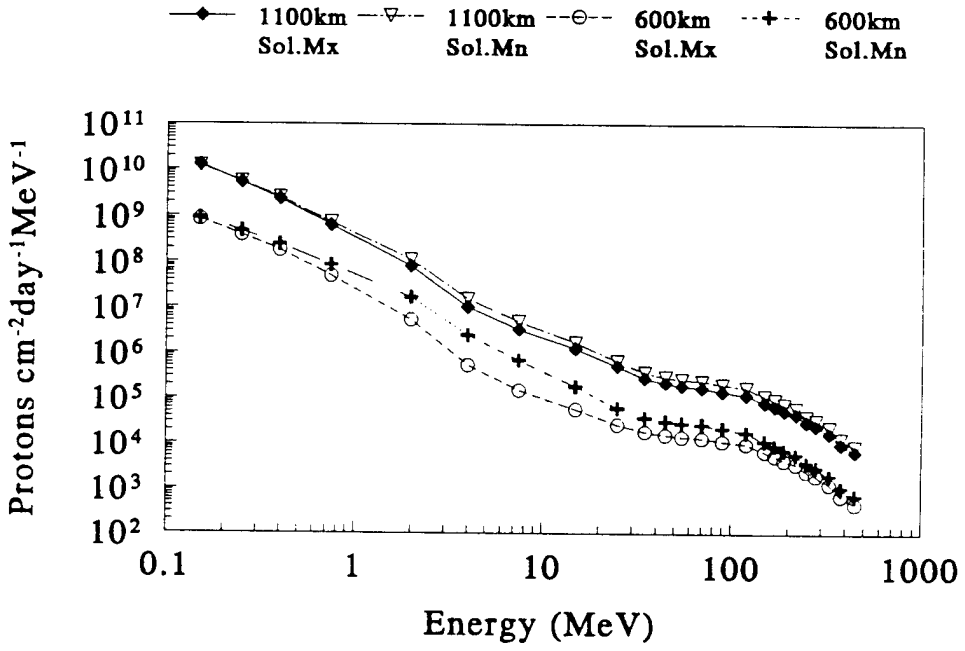

Figure 2. Trapped differential proton spectra.

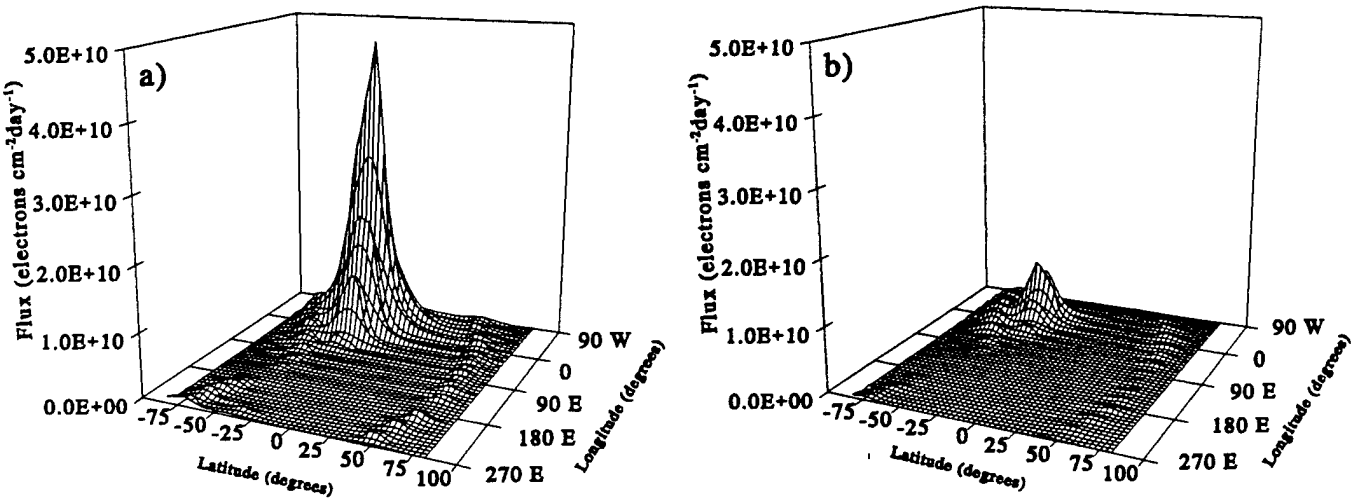

Figure 3. Spatial distribution of the trapped electron flux at the 1100km altitude (a) and the 600 km altitude (b).

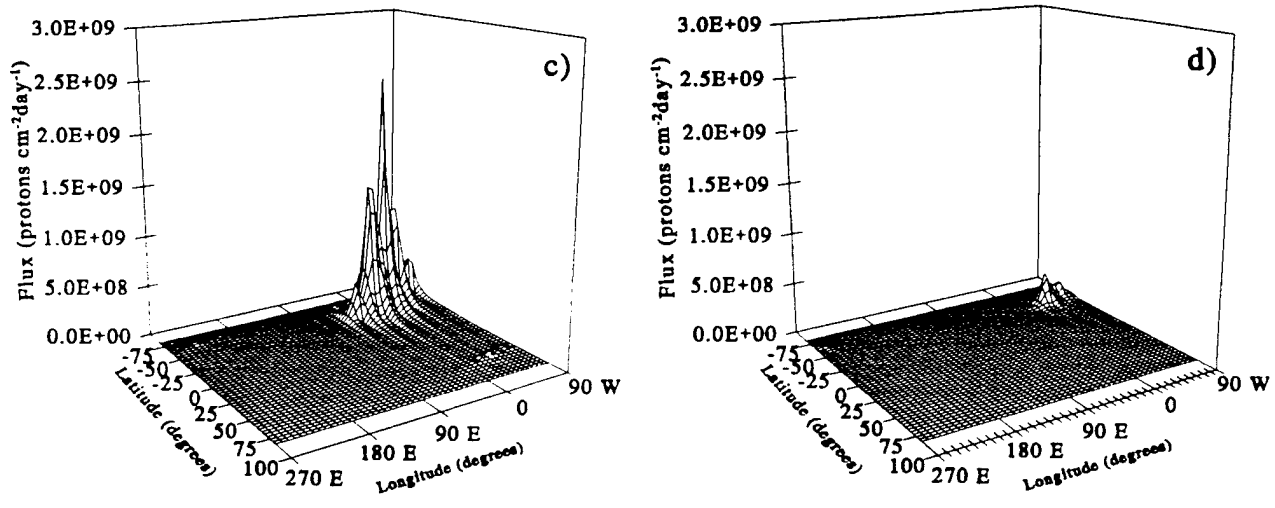

Figure 4. Spatial distribution of the trapped proton flux at the 1100km altitude (c) and the 600km altitude (d).

3. COSMIC RAYS

There are two cosmic ray components that affect the total radiation dose received by an earth-orbiting spacecraft, namely the galactic component and solar component. Galactic cosmic rays, originating outside the solar system, are relatively low fluxes of ions having energies extending beyond the TeV energy range and include all elements found in the periodic table. The solar cosmic rays are of solar flare origin. These are energetic protons, with a minor component of alpha particles, heavy ions, and electrons. The maximum energy is several hundred MeV. Solar coronal holes are also a source of this type of radiation.

The cosmic ray radiation contribution to the total dose received by an earth-orbiting satellite platform can be predicted with the use of the CREME code[2]. In determining the various particle spectra, CREME makes use of experimental data from a variety of sources. For example, in-situ measured spectra of cosmic ray protons and alpha particles are scaled by appropriate factors[2] to determine particle spectra for heavier elements, up to Ni in the periodic table. The values of these scaling factors were deduced from the element-abundance measurements originating from a French-Danish experiment[3], taken on-board HEAO-3. To obtain spectra of ionized elements heavier than Ni, scaling factors are also applied to measured iron spectra and other heavy nuclei, from the heavy nuclei experiment[4,5,6], also taken on-board HEAO-3.

Cosmic ray spectra for Proton, Helium, Oxygen, and Iron for the 600km altitude orbit are shown in Figures 5 and 6. Figures 7 and 8 show the spectra for the same elements but for the 1100km altitude orbit. CREME classifies the space environment into twelve categories each called an "Interplanetary Weather Index" (IWI). The weather indices numbered 1 to 4 relate to galactic cosmic rays of various intensity and composition. The other 8 (numbered 5 to 12, inclusive) also include solar flare cosmic rays of various compositions and intensities[2]. The solar component is the dominating factor in the cosmic ray spectrum. This is evident when one compares plots in Figures 5 and 6 or plots in Figures 7 and 8. Tables 3,4,5, and 6 provide numerical summary of the calculations.

4. LET SPECTRUM

Integral LET spectra for the 1100km altitude orbit (Figure 9) and the 600km altitude orbit (Figure 10) have been calculated for various space radiation scenarios based on the space environment characterization scheme in CREME. The plot labeled IWI=1 is the LET spectrum of the average galactic cosmic rays, while IWI=3 plot is the LET spectrum of the so called "worst case" galactic cosmic rays. Curves IWI=6 and 8 are LET spectra of the galactic cosmic rays plus the solar component. The solar component in the IWI=6 plot is an average intensity solar flare while for the IWI=8 curve, the solar flare component ranks at the top 10% of the most intense solar flares. These two cases (IWI=6 and 8) are also referred to as worst case composition environments, as opposed to the average composition IWI=5 and IWI=7 (not shown). The average and worst case composition differ in the relative intensity of heavy ions with respect to the proton component in the spectrum. The IWI=10 curve relates to August 1972 solar flare.

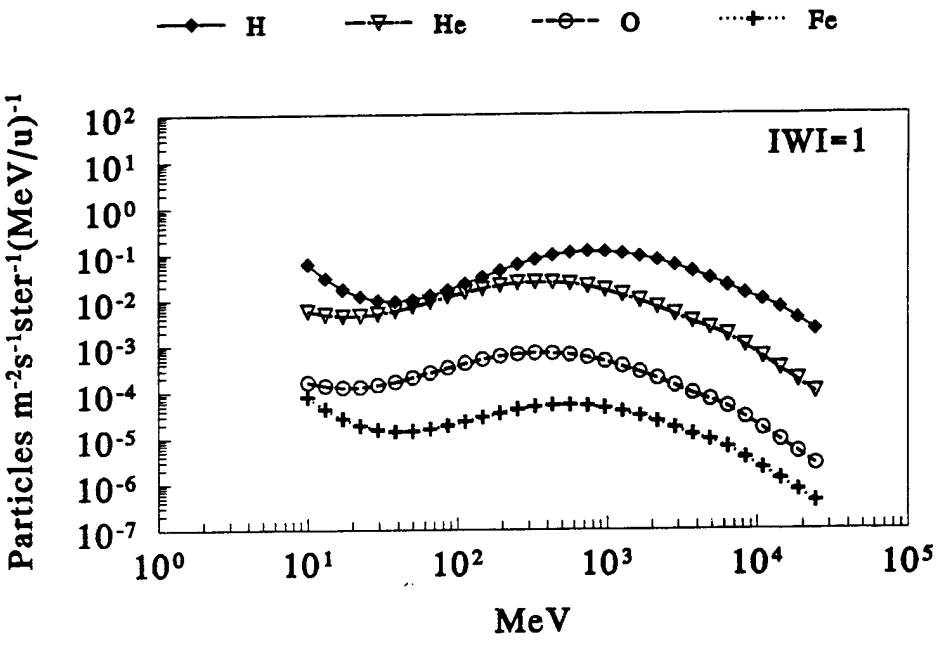

Figure 5. Proton, Helium, Oxygen and Iron spectra for galactic cosmic rays at the altitude of 600km.

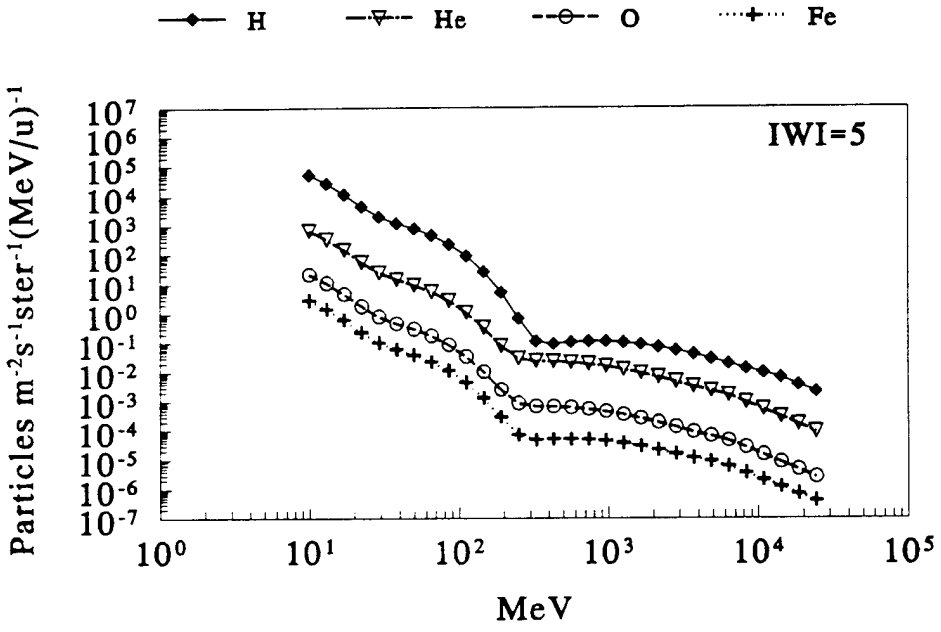

Figure 6. Proton, Helium, Oxygen and Iron spectra for galactic cosmic rays plus an average solar flare particle flux at the altitude of 600km.

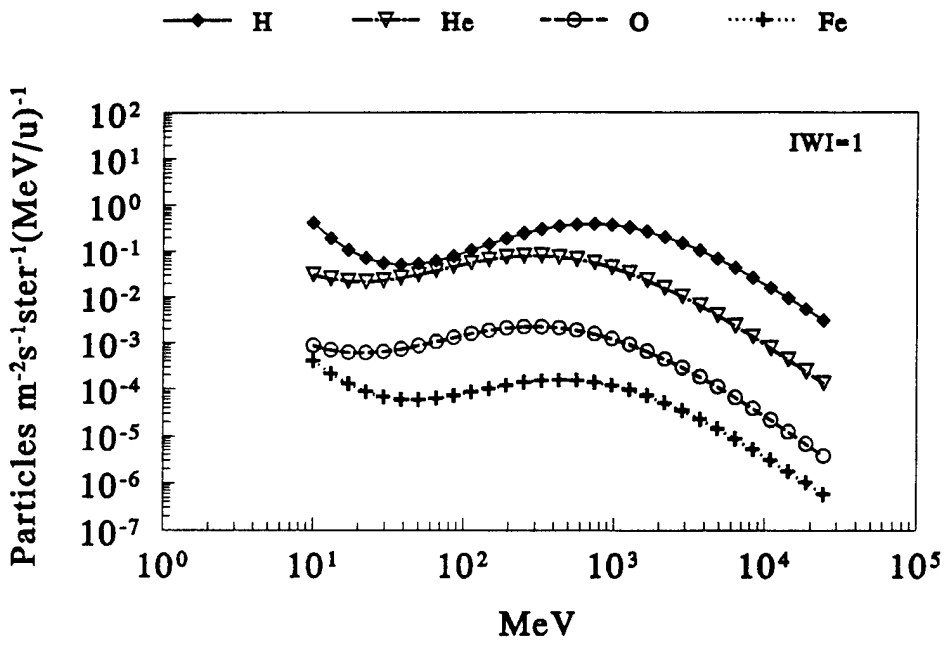

Figure 7. Proton, Helium, Oxygen and Iron spectra for galactic cosmic rays at the altitude of 1100km.

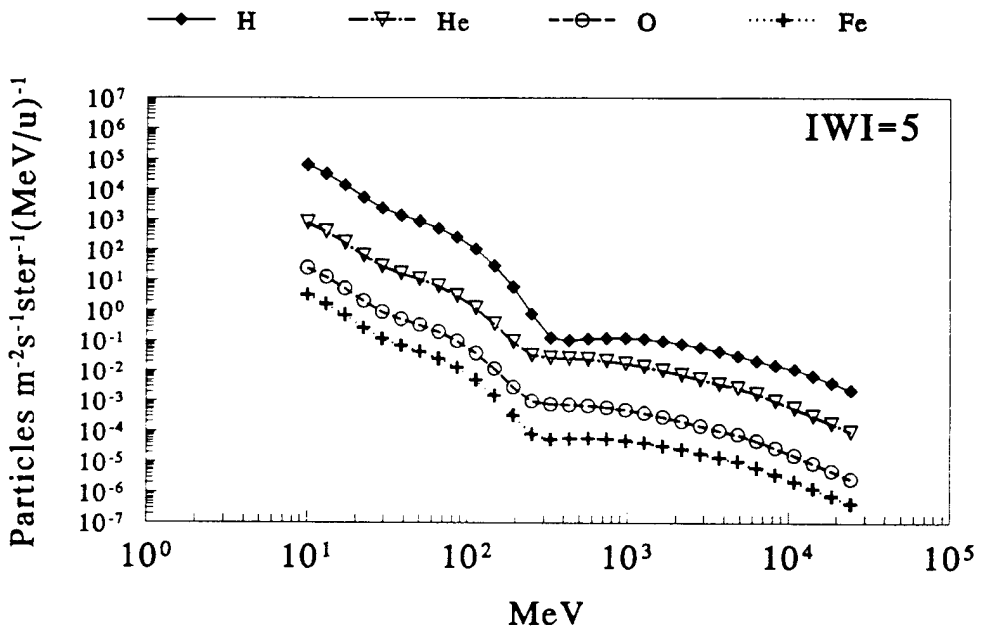

Figure 8. Proton, Helium, Oxygen and Iron spectra for galactic cosmic rays plus an average solar flare particle flux at the altitude of 1100km.

Table 3. Differential galactic cosmic ray flux (particles m^{-2} s^{-1} $ster^{-1}$ $(MeV/u)^{-1}$) at the altitude of 600km (four elements shown).

Energy(MeV)	H	He	O	Fe
1.00E+01	6.05E-02	5.68E-03	1.61E-04	7.81E-05
1.50E+01	2.20E-02	4.55E-03	1.29E-04	3.31E-05
2.24E+01	1.18E-02	4.50E-03	1.28E-04	1.87E-05
3.36E+01	9.25E-03	5.34E-03	1.52E-04	1.42E-05
5.02E+01	1.01E-02	7.15E-03	2.03E-04	1.40E-05
7.52E+01	1.40E-02	1.02E-02	2.91E-04	1.68E-05
1.13E+02	2.23E-02	1.45E-02	4.12E-04	2.25E-05
1.69E+02	3.67E-02	1.91E-02	5.44E-04	3.11E-05
2.52E+02	5.84E-02	2.28E-02	6.47E-04	4.11E-05
3.78E+02	8.38E-02	2.39E-02	6.79E-04	4.92E-05
5.66E+02	1.04E-01	2.18E-02	6.20E-04	5.16E-05
8.47E+02	1.11E-01	1.75E-02	4.97E-04	4.71E-05
1.27E+03	1.01E-01	1.25E-02	3.54E-04	3.72E-05
1.90E+03	7.92E-02	7.99E-03	2.27E-04	2.58E-05
2.84E+03	5.48E-02	4.70E-03	1.33E-04	1.62E-05
4.25E+03	3.40E-02	2.68E-03	7.62E-05	1.01E-05
6.37E+03	1.94E-02	1.62E-03	4.61E-05	6.06E-06
9.54E+03	1.09E-02	7.18E-04	2.04E-05	2.78E-06
1.43E+04	6.44E-03	3.03E-04	8.61E-06	1.23E-06
2.14E+04	2.81E-03	1.24E-04	3.53E-06	5.36E-07

Table 4. Differential galactic cosmic rays flux including an average intensity solar flare component (particles m^{-2} s^{-1} $ster^{-1}$ $(MeV/u)^{-1}$) at the altitude of 600km (four elements shown).

Energy(MeV)	H	He	O	Fe
1.00E+01	5.42E+04	6.74E+02	2.16E+01	2.83E+00
1.50E+01	1.81E+04	2.25E+02	7.21E+00	9.43E-01
2.24E+01	4.48E+03	5.53E+01	1.77E+00	2.31E-01
3.36E+01	1.47E+03	1.82E+01	5.81E-01	7.57E-02
5.02E+01	7.61E+02	9.24E+00	2.96E-01	3.87E-02
7.52E+01	3.25E+02	3.94E+00	1.26E-01	1.65E-02
1.13E+02	8.87E+01	1.08E+00	3.46E-02	4.48E-03
1.69E+02	1.23E+01	1.67E-01	5.26E-03	6.46E-04
2.52E+02	6.78E-01	3.02E-02	8.84E-04	7.20E-05
3.78E+02	9.07E-02	2.40E-02	6.82E-04	4.95E-05
5.66E+02	1.04E-01	2.18E-02	6.20E-04	5.16E-05
8.47E+02	1.11E-01	1.75E-02	4.97E-04	4.71E-05
1.27E+03	1.01E-01	1.25E-02	3.54E-04	3.72E-05
1.90E+03	7.92E-02	7.99E-03	2.27E-04	2.58E-05
2.84E+03	5.48E-02	4.70E-03	1.33E-04	1.62E-05
4.25E+03	3.40E-02	2.68E-03	7.62E-05	1.01E-05
6.37E+03	1.94E-02	1.62E-03	4.61E-05	6.06E-06
9.54E+03	1.09E-02	7.18E-04	2.04E-05	2.78E-06
1.43E+04	6.44E-03	3.03E-04	8.61E-06	1.23E-06
2.14E+04	2.81E-03	1.24E-04	3.53E-06	5.36E-07

Table 5. Differential galactic cosmic rays flux (particles m^{-2} s^{-1} $ster^{-1}$ $(MeV/u)^{-1}$) at the altitude of 1100km (four elements shown).

Energy(MeV)	H	He	O	Fe
1.00E+01	7.21E-02	6.64E-03	1.89E-04	9.11E-05
1.50E+01	2.60E-02	5.29E-03	1.50E-04	3.84E-05
2.24E+01	1.39E-02	5.20E-03	1.48E-04	2.16E-05
3.36E+01	1.08E-02	6.16E-03	1.75E-04	1.63E-05
5.02E+01	1.18E-02	8.26E-03	2.35E-04	1.61E-05
7.52E+01	1.63E-02	1.17E-02	3.34E-04	1.92E-05
1.13E+02	2.58E-02	1.66E-02	4.70E-04	2.58E-05
1.69E+02	4.24E-02	2.18E-02	6.20E-04	3.55E-05
2.52E+02	6.70E-02	2.60E-02	7.37E-04	4.68E-05
3.78E+02	9.55E-02	2.71E-02	7.70E-04	5.60E-05
5.66E+02	1.19E-01	2.48E-02	7.05E-04	5.87E-05
8.47E+02	1.26E-01	1.99E-02	5.66E-04	5.35E-05
1.27E+03	1.15E-01	1.42E-02	4.03E-04	4.22E-05
1.90E+03	8.98E-02	9.04E-03	2.57E-04	2.92E-05
2.84E+03	6.21E-02	5.37E-03	1.53E-04	1.86E-05
4.25E+03	3.85E-02	3.30E-03	9.36E-05	1.25E-05
6.37E+03	2.22E-02	1.77E-03	5.03E-05	6.56E-06
9.54E+03	1.35E-02	7.77E-04	2.21E-05	3.01E-06
1.43E+04	6.97E-03	3.28E-04	9.32E-06	1.34E-06
2.14E+04	3.04E-03	1.35E-04	3.83E-06	5.80E-07

Table 6. Differential galactic cosmic rays flux including an average intensity solar flare component (particles m^{-2} s^{-1} $ster^{-1}$ $(MeV/u)^{-1}$ at the altitude of 1100km (four elements shown).

Energy(MeV)	H	He	O	Fe
1.00E+01	6.46E+04	7.88E+02	2.52E+01	3.30E+00
1.50E+01	2.15E+04	2.62E+02	8.38E+00	1.09E+00
2.24E+01	5.28E+03	6.40E+01	2.05E+00	2.67E-01
3.36E+01	1.73E+03	2.10E+01	6.71E-01	8.74E-02
5.02E+01	8.87E+02	1.07E+01	3.41E-01	4.45E-02
7.52E+01	3.76E+02	4.52E+00	1.45E-01	1.89E-02
1.13E+02	1.02E+02	1.24E+00	3.95E-02	5.13E-03
1.69E+02	1.42E+01	1.90E-01	6.00E-03	7.38E-04
2.52E+02	7.77E-01	3.44E-02	1.01E-03	8.21E-05
3.78E+02	1.03E-01	2.72E-02	7.73E-04	5.64E-05
5.66E+02	1.19E-01	2.48E-02	7.05E-04	5.87E-05
8.47E+02	1.26E-01	1.99E-02	5.66E-04	5.35E-05
1.27E+03	1.15E-01	1.42E-02	4.03E-04	4.22E-05
1.90E+03	8.98E-02	9.04E-03	2.57E-04	2.92E-05
2.84E+03	6.21E-02	5.37E-03	1.53E-04	1.86E-05
4.25E+03	3.85E-02	3.30E-03	9.36E-05	1.25E-05
6.37E+03	2.22E-02	1.77E-03	5.03E-05	6.56E-06
9.54E+03	1.35E-02	7.77E-04	2.21E-05	3.01E-06
1.43E+04	6.97E-03	3.28E-04	9.32E-06	1.34E-06
2.14E+04	3.04E-03	1.35E-04	3.83E-06	5.80E-07

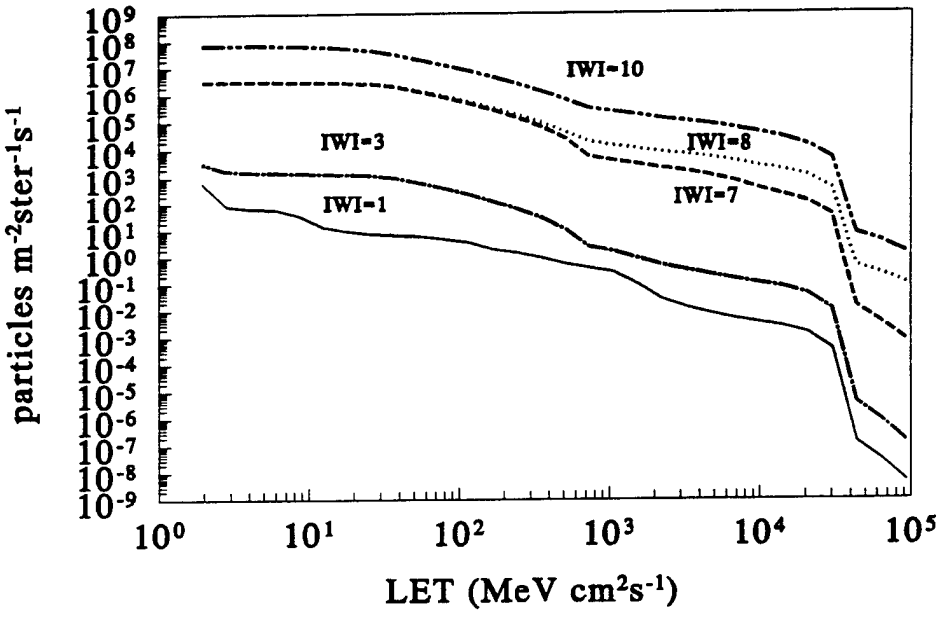

Figure 9. LET spectrum plots for specified interplanetary conditions for the 600km circular orbit.

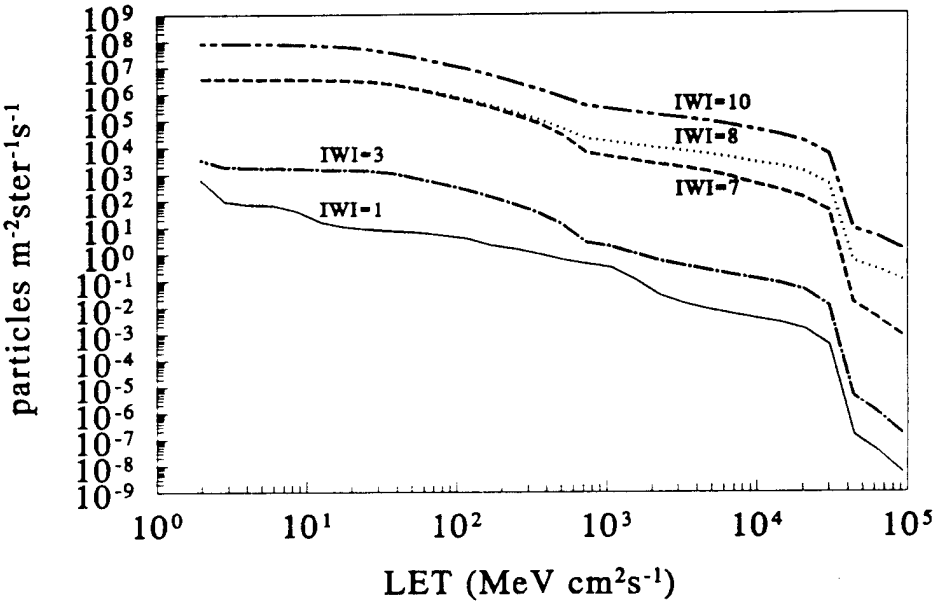

Figure 10. LET spectrum plots for specified interplanetary conditions for the 1100km circular orbit.

5. SHIELDING EFFECT ON LET SPECTRUM

The effect of Aluminum shielding on the LET spectrum for the two orbits has been investigated. Aluminum thicknesses of 1mm, 3mm, and 5mm were used for this purpose. The results are shown in Figures 11 and 12 (600km-altitude orbit) and Figures 13 and 14 (1100km altitude orbit). Figures 11 and 13 relate to galactic cosmic rays only, while Figures 12 and 14 show the shielding effect on LET spectrum due to the galactic cosmic rays containing an ordinary solar flare component. The unshielded LET spectrum is also shown for a comparison purpose. It is evident that shielding is more effective in the case where the solar component is present.

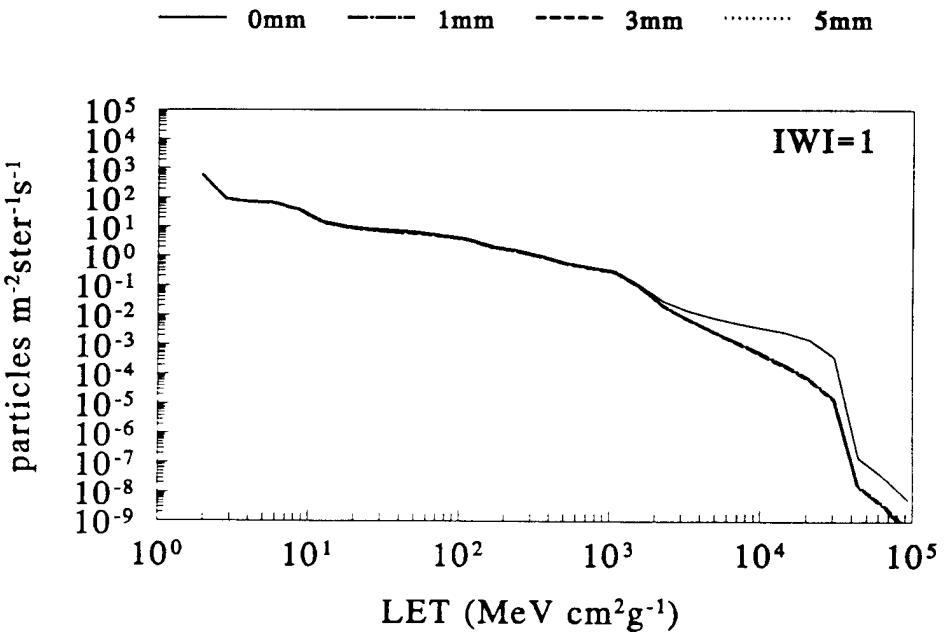

Figure 11. Effect of Aluminum shielding thickness on the LET spectrum of galactic cosmic rays at the altitude of 600km.

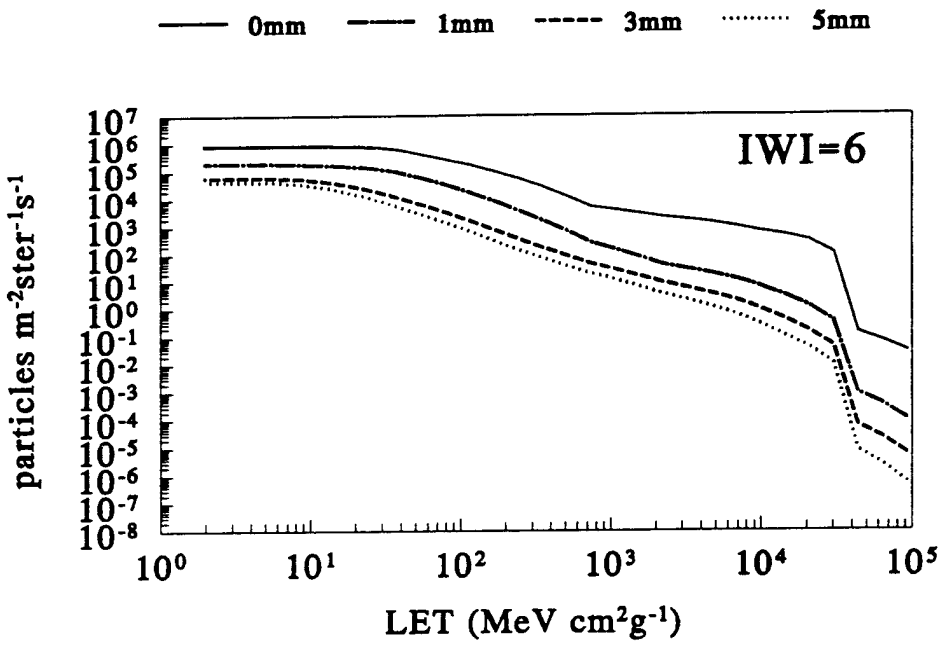

Figure 12. Effect of Aluminum shielding on the LET spectrum of galactic cosmic rays including an average intensity solar flare component at the altitude of 600km.

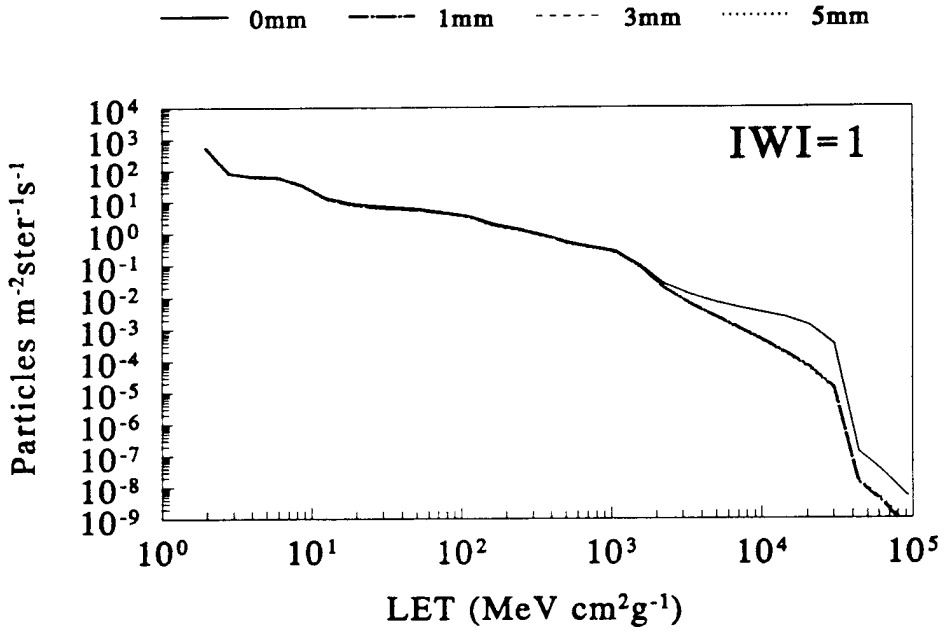

Figure 13. Effect of Aluminum shielding thickness on the LET spectrum of galactic cosmic rays at the altitude of 1100km.

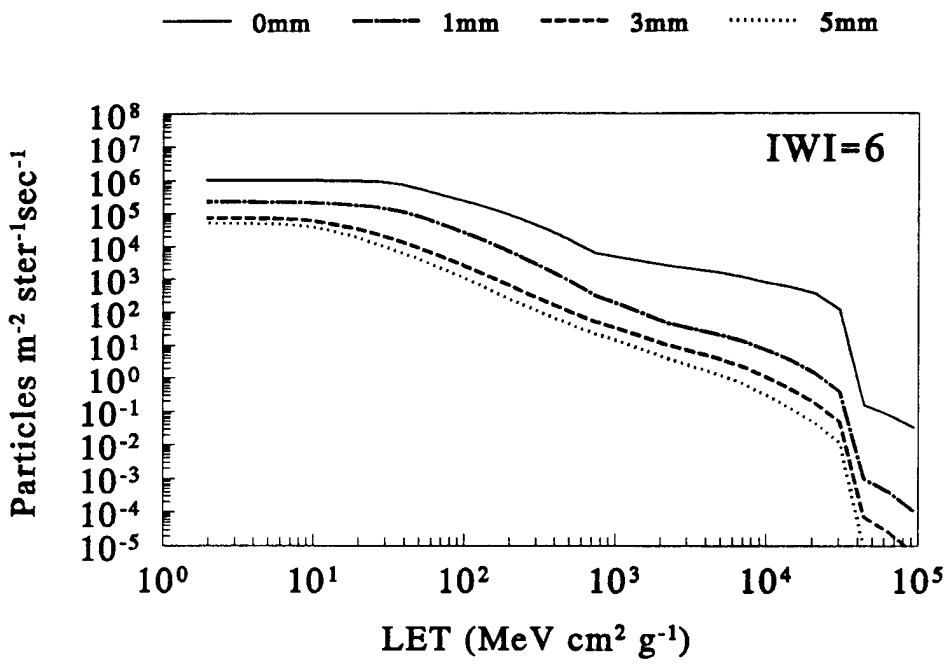

Figure 14. Effect of Aluminum shielding on the LET spectrum of galactic cosmic rays including an average intensity solar flare component at the altitude of 1100km.

6. UPSET RATES.

The number and the magnitude of solar flares experienced by a satellite can significantly influence estimates of both the upset rates and the total mission radiation dose. Other parameters affecting upset rates include the sensitive volume of the device (referring to a region of the device containing an electric field), the critical charge (the amount of charge required to change the state of the device), and the shielding thickness.

Using CREME, upset rate calculation results as a function of sensitive volume size and critical charge magnitude are shown in Figure 15. For this example, the 1100km altitude orbit and an IWI value of 3 have been selected. The plots relate the size of the sensitive volume (selected to be equal to 1000, 1.0, and 0.125 microns cube) and the size of the critical charge with the upset rate.

The effect of solar activity and the shielding thickness for the 1100km altitude orbit on the upset rates is shown in Figure 16. Here the critical charge and the critical volume parameters were 1pC and 1 cubic micron respectively. It is worth noting that shielding thickness is less effective in the pure galactic cosmic ray environment. The same plot for the 600km altitude orbit is shown in Figure 17.

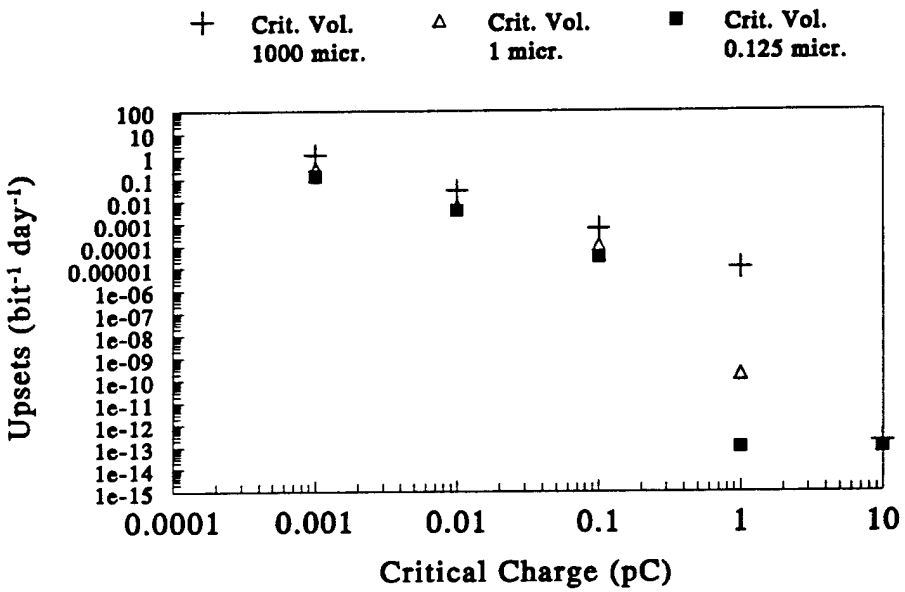

Figure 15. The critical volume size and the critical charge magnitude effect on device upset rates at 1100km altitude.

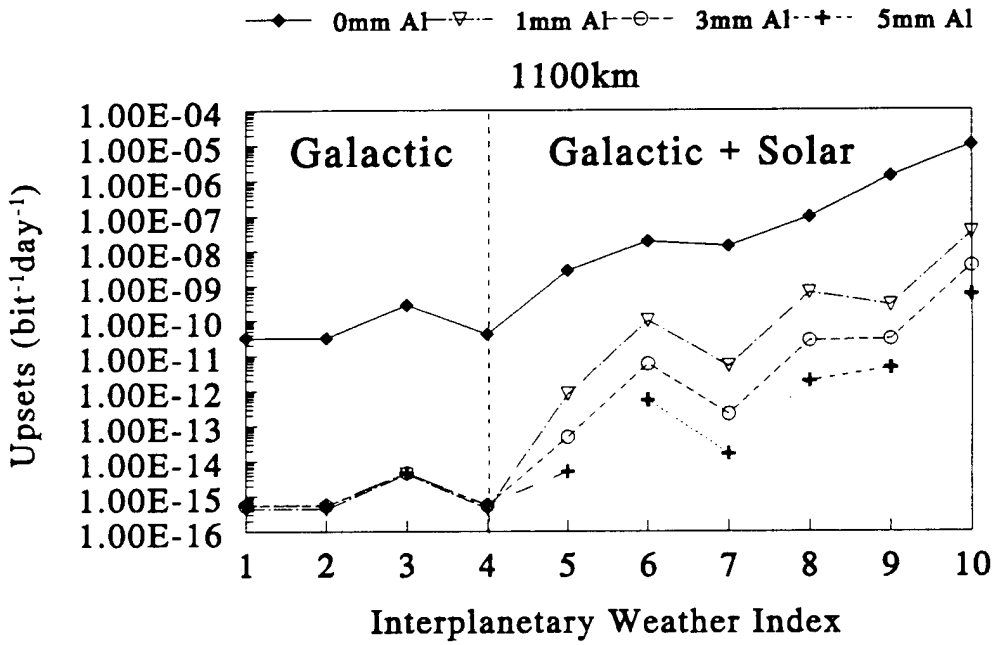

Figure 16. Shielding and solar activity effect on device upset rates at the 1100km altitude.

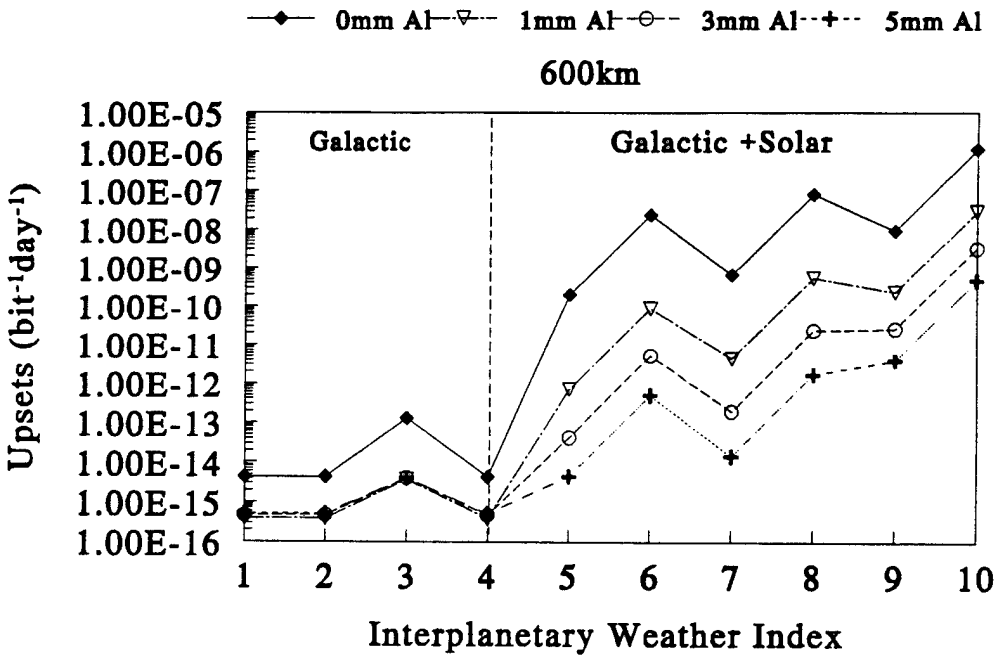

Figure 17. Shielding and solar activity effect on device upset rates at the 600km altitude.

7. DOSE DEPOSITION

A three dimensional Monte Carlo N-Particle (MCNP) code has been used to determine the dose delivered into a silicon detector by the electrons and protons for the two orbits. Both trapped and cosmic ray components were used in the calculations. In the scenario IWI=5, the dose due to protons also includes a contribution from an average intensity solar flare. The detector was a thin silicon shell surrounded by a spherical shielding with thickness ranging from 1mm to 9mm. A case without shielding is also given in Table 7.

Table 7. Dose deposition rates (rad day^{-1}) at the 600km-altitude orbit.

Aluminum Shielding (mm)	IWI=1			IWI=5		
	Electrons	Protons	Total	Electrons	Protons + Solar Flare	Total
0	2.118E+03	2.202E+02	2.338E+03	2.118E+03	2.420E+02	2.360E+03
1	1.549E+01	1.770E+00	1.726E+01	1.549E+01	1.819E+01	3.369E+01
2	4.174E+00	1.199E+00	5.373E+00	4.174E+00	5.180E+00	9.353E+00
3	1.423E+00	1.030E+00	2.453E+00	1.423E+00	3.553E+00	4.976E+00
4	5.292E-01	9.124E-01	1.442E+00	5.292E-01	2.540E+00	3.069E+00
5	2.035E-01	8.486E-01	1.052E+00	2.035E-01	2.221E+00	2.425E+00
6	8.323E-02	7.497E-01	8.329E-01	8.323E-02	1.686E+00	1.769E+00
7	3.470E-02	7.106E-01	7.453E-01	3.470E-02	1.560E+00	1.595E+00
8	1.904E-02	6.742E-01	6.933E-01	1.904E-02	1.421E+00	1.440E+00
9	1.349E-02	6.091E-01	6.226E-01	1.349E-02	1.175E+00	1.188E+00

Table 8. Dose deposition rates (rad day^{-1}) at the 1100km-altitude orbit.

Aluminum Shielding (mm)	IWI=1			IWI=5		
	Electrons	Protons	Total	Electrons	Protons + Solar Flare	Total
0	1.481E+04	1.934E+03	1.674E+04	1.481E+04	1.959E+03	1.677E+04
1	5.019E+01	1.413E+01	6.432E+01	5.019E+01	3.244E+01	8.263E+01
2	1.234E+01	8.976E+00	2.132E+01	1.234E+01	1.335E+01	2.569E+01
3	4.177E+00	7.544E+00	1.172E+01	4.177E+00	1.043E+01	1.461E+01
4	1.549E+00	6.580E+00	8.128E+00	1.549E+00	8.533E+00	1.008E+01
5	5.881E-01	6.123E+00	6.712E+00	5.881E-01	7.765E+00	8.353E+00
6	2.500E-01	5.416E+00	5.666E+00	2.500E-01	6.524E+00	6.773E+00
7	1.181E-01	5.138E+00	5.256E+00	1.181E-01	6.150E+00	6.268E+00
8	7.558E-02	4.878E+00	4.954E+00	7.558E-02	5.780E+00	5.855E+00
9	6.028E-02	4.413E+00	4.473E+00	6.028E-02	5.122E+00	5.183E+00

The radiation source in the model was distributed over the surface of the detector/shielding assembly, however, the direction of the emission was non-isotropic (directed toward the geometrical centre the detector)

8. SUMMARY

In this work, we have used the AE8, AP8, and CREME space environment codes to obtain an estimate for the electron and proton flux data for the 600km altitude and 1100km altitude orbits. LET and effect of shielding on LET spectra for the two orbits were also calculated. The upset rates were also estimated for various solar flare activity scenarios.

For the dose rate calculations, a three-dimensional Monte Carlo N-Particle (MCNP) code was used. The nature of the source used does not exactly reflect the directionality of the space radiation and hence one would expect that the dose rate results calculated would differ somewhat from the results one would obtain with the isotropic source

9. REFERENCES

1. C.E. McIlwain, "Coordinates for Mapping the Distribution of Magnetically Trapped Particles", J. Geophys. Res., 66, 3681-1691, 1961.

2. J.H. Adams Jr., "Cosmic Ray Effects on Microelectronics, Part IV", NRL Memorandum Report 5901, December 1987.

3. J.J. Engelmann, A.J. Simpson, E. Juliusson, L. Koch-Miramond, P. Masse, A. Soutol, B. Byrnak, N. Lund, B. Peters, I.L. Rassmussen, M. Rotenberg, N.J. Westergaard, "Elemental Composition of Cosmic Rays from Be to Ni as Measured by the French-Danish Instrument on HEAO-3", Proceedings of the 18th Inter. Cos. Ray Conf., Vol. 2, 17-20, Bangalore, India, 1983.

4. W.R. Binns, R.K. Fickle, T.L. Garrard, M.H. Israel, J. Klarmann, E.C. Stone, C.J. Waddington, "Cosmic Ray Abundances of Elements with Atomic Numbers 26<Z<40", Astrophysical Journal, Vol. 247, 1982.

5. W.R. Binns, R.K. Fickle, T.L. Garrard, M.H. Israel, J. Klarmann, E.C. Stone, C.J. Waddington, "The Abundance of Actinides in the Cosmic Radiation as Measured on HEAO-3", Astrophysical Journal, Vol. 261, 1982.

6. W.R. Binns, R.K. Fickle, T.L. Garrard, M.H. Israel, J. Klarmann, K.E. Krombel, E.C. Stone, C.J. Waddington, "Cosmic Ray Abundances of Sn, Te, Xe, and Ba Nuclei Measured on HEAO-3", Astrophysical Journal, Vol. 267, 1983.

UNCLASSIFIED
SECURITY CLASSIFICATION OF FORM
(highest classification of Title, Abstract, Keywords)

DOCUMENT CONTROL DATA

(Security classification of title, body of abstract and indexing annotation must be entered when the overall document is classified)

1. ORIGINATOR (the name and address of the organization preparing the document. Organizations for whom the document was prepared, e.g. Establishment sponsoring a contractor's report, or tasking agency, are entered in section 8.)

Defence Research Establishment Ottawa
3701 Carling Ave, Ottawa, K1A 0Z4 Canada

2. SECURITY CLASSIFICATION (overall security classification of the document, including special warning terms if applicable)

UNCLASSIFIED

3. TITLE (the complete document title as indicated on the title page. Its classification should be indicated by the appropriate abbreviation (S,C or U) in parentheses after the title.)

Analysis of the Radiation Environment Effects on Electronic Components in Near-Earth Orbits (U)

4. AUTHORS (Last name, first name, middle initial)

Varga, L., Horvath, E. B., and Cousins, T.

5. DATE OF PUBLICATION (month and year of publication of document)	6a. NO. OF PAGES (total containing information. Include Annexes, Appendices, etc.)	6b. NO. OF REFS (total cited in document)
November 2000	26	6

7. DESCRIPTIVE NOTES (the category of the document, e.g. technical report, technical note or memorandum. If appropriate, enter the type of report, e.g. interim, progress, summary, annual or final. Give the inclusive dates when a specific reporting period is covered.)

Technical Memorandum

8. SPONSORING ACTIVITY (the name of the department project office or laboratory sponsoring the research and development. Include the address.)

9a. PROJECT OR GRANT NO. (if appropriate, the applicable research and development project or grant number under which the document was written. Please specify whether project or grant)	9b. CONTRACT NO. (if appropriate, the applicable number under which the document was written)
5EC12	

10a. ORIGINATOR'S DOCUMENT NUMBER (the official document number by which the document is identified by the originating activity. This number must be unique to this document.)	10b. OTHER DOCUMENT NOS. (Any other numbers which may be assigned this document either by the originator or by the sponsor)
DREO TECHNICAL MEMORANDUM 2000-071	

11. DOCUMENT AVAILABILITY (any limitations on further dissemination of the document, other than those imposed by security classification)

(X) Unlimited distribution
( ) Distribution limited to defence departments and defence contractors; further distribution only as approved
( ) Distribution limited to defence departments and Canadian defence contractors; further distribution only as approved
( ) Distribution limited to government departments and agencies; further distribution only as approved
( ) Distribution limited to defence departments; further distribution only as approved
( ) Other (please specify):

12. DOCUMENT ANNOUNCEMENT (any limitation to the bibliographic announcement of this document. This will normally correspond to the Document Availability (11). However, where further distribution (beyond the audience specified in 11) is possible, a wider announcement audience may be selected.)

UNCLASSIFIED
SECURITY CLASSIFICATION OF FORM

13. ABSTRACT (a brief and factual summary of the document. It may also appear elsewhere in the body of the document itself. It is highly desirable that the abstract of classified documents be unclassified. Each paragraph of the abstract shall begin with an indication of the security classification of the information in the paragraph (unless the document itself is unclassified) represented as (S), (C), or (U). It is not necessary to include here abstracts in both official languages unless the text is bilingual).

ABSTRACT

The radiation environments at two low altitude orbits have been calculated with the NASA space environment models and codes AP8/AE8, Vette, and CREME. LET spectra and device upset rates for various solar activity scenarios have been determined. Dose deposition into silicon targets as a function of Aluminum shielding thickness has been also calculated with a Monte Carlo code. The results indicate that parameters such as orbit altitude, shielding thickness, and solar activity strongly affect the SEU rates.

RÉSUMÉ

L'environnement de rayonnement à deux orbites de basse altitude a été calculé en utilisant des modèles d'environnement e l'espace de NASA's et code AP8/AE8, Vette et CRÈME. Les spectres LET et les cadences bouleversées de dispositif pour différents scénarios solaires d'activité avoir été déterminé. Le dépôt de dose dans des cibles de silicium en fonction d'épaisseur d' armature d'aluminium a été également calculé en utilisant un code de Monte Carlo. Les résultats indiquent que les paramètres tels que l'altitude d'orbite, protégeant l'épaisseur et l'activité solaire affectent fortement les
cadences de SEU.

14. KEYWORDS, DESCRIPTORS or IDENTIFIERS (technically meaningful terms or short phrases that characterize a document and could be helpful in cataloguing the document. They should be selected so that no security classification is required. Identifiers such as equipment model designation, trade name, military project code name, geographic location may also be included. If possible keywords should be selected from a published thesaurus. e.g. Thesaurus of Engineering and Scientific Terms (TEST) and that thesaurus-identified. If it is not possible to select indexing terms which are Unclassified, the classification of each should be indicated as with the title.)

Space Radiation Environment, Trapped Radiation, Low-Earth Orbit, Space Environment Code, Monte Carlo Code, Solar Activity, Satellite Electronic Components, LET Spectrum, Dose Deposition, Upset Rates

Defence R&D Canada
is the national authority for providing
Science and Technology (S&T) leadership
in the advancement and maintenance
of Canada's defence capabilities.

R et D pour la défense Canada
est responsable, au niveau national, pour
les sciences et la technologie (S et T)
au service de l'avancement et du maintien des
capacités de défense du Canada.

www.drdc-rddc.dnd.ca